

## Microphysical Structure of Winter Monsoon Cloud Clusters<sup>1</sup>

ROBERT A. HOUZE, JR., AND DEAN D. CHURCHILL

*Department of Atmospheric Sciences, University of Washington, Seattle, WA 98195*

(Manuscript received 3 January 1984, in final form 13 August 1984)

### ABSTRACT

Images of hydrometeors in the size range 0.1 to 1.6 mm were obtained by aircraft in precipitating clouds over the South China Sea during Winter MONEX. These observations document for the first time the particle structures and concentrations in tropical cloud clusters above the 0°C level. The data were obtained under nearly constant atmospheric conditions (altitude 7–8 km, temperature –14 to –19°C). The particle samples were stratified according to the type of precipitation in which they were observed as determined from airborne radar, and according to particle size and shape.

The convective cells in the observed clusters were not unlike cells observed elsewhere. They had typical particle concentrations of 100–300 per liter, and riming was apparently the dominant growth mechanism. Ice multiplication may have been active in the convection.

The stratiform regions of the clusters were microphysically quite distinct from the convective cells. “Strong” stratiform precipitation areas (radar reflectivity greater than 20 dBZ) had typical concentrations of 20–70 per liter, while “weak” stratiform precipitation characterized by reflectivities of 1–20 dBZ and “very weak” stratiform precipitation (reflectivities less than 1 dBZ) had concentrations almost exclusively less than 10 per liter. Vapor grown crystals were found in the stratiform regions. The habits of these vapor grown crystals were consistent with the presence of mesoscale updraft. Particles whose crystal habits could not be definitely identified were referred to as “indeterminable.” In the stratiform regions, the presence of many indeterminable ice particles suggested (but did not prove) that aggregation of ice crystals was an important particle growth mechanism. “Very weak” stratiform precipitation regions exhibited characteristics of dissipating stratiform clouds.

### 1. Introduction

Most precipitation near the equator occurs in “cloud clusters,” which are identified by their distinctive mesoscale upper-level cloud shield seen in satellite imagery. Field experiments such as GATE and MONEX<sup>2</sup> have provided observations of the precipitation structure of cloud clusters (see reviews by Houze and Betts, 1981; Houze and Hobbs, 1982). Radar data obtained in these experiments show that the precipitation within intense cloud clusters can be subdivided into convective and stratiform regions, with some 30–50% of the total precipitation falling in the stratiform regions (Houze, 1977; Gamache and Houze, 1983; Houze and Rappaport, 1984; Churchill and Houze, 1984a; Leary, 1984).

Relatively little is known about the microphysical structure of tropical cloud clusters. Raindrop size distributions observed in GATE have been studied to obtain relationships among radar reflectivity, rainwater content of the air, and surface rainfall rate

(Cunning and Sax, 1977; Austin and Geotis, 1979). Leary (1980) used the GATE observed raindrop size distributions to deduce mesoscale downdraft motion and evaporation rates below cloud base in the stratiform regions of GATE cloud clusters. Leary and Houze (1979) used these raindrop size distributions to infer the probable nature of ice particles occurring above the melting layer in the stratiform regions; however, *in situ* observations of the particles above the 0°C level have never been made prior to MONEX.

Direct observations of particles at subzero temperatures were obtained in cloud clusters during Winter MONEX<sup>3</sup> with two-dimensional Particle Measurement System (PMS) probes aboard a NOAA WP-3D aircraft. Churchill and Houze (1984a) examined these data in a case study of cloud clusters that occurred over the South China Sea on 10 December 1978.

During Winter MONEX, the WP-3D aircraft was used primarily as a dropwindsonde platform, so most flights were at altitudes of 7–8 km. This nearly constant flight level, maintained throughout the ex-

<sup>1</sup> Contribution Number 718 from the Department of Atmospheric Sciences, University of Washington.

<sup>2</sup> GATE and MONEX were the Global Atmospheric Research Programme's Atlantic Tropical and Monsoon Experiments, respectively.

<sup>3</sup> MONEX was divided into Winter MONEX, staged over Indonesia, Malaysia and surrounding seas during December 1978–February 1979, and Summer MONEX, which was held over India, the Arabian Sea and the Bay of Bengal during June–July 1979.

periment, provided microphysical sampling at nearly uniform atmospheric conditions (generally  $-14$  to  $-19^{\circ}\text{C}$ ) in nine different clusters over the South China Sea. In the three clusters sampled on 10 December, Churchill and Houze (1984a) found that at these altitudes in the regions of convective precipitation, active cells contained particles in concentrations of the order of hundreds per liter, and the dominant growth mechanism appeared to be riming. In the stratiform regions of clusters, particle concentrations were one to two orders of magnitude lower than in the convective regions; areas of weaker stratiform precipitation had concentrations 1–10 per liter, while areas of stronger stratiform precipitation generally had between 10 and 100 per liter. The dominant particle growth mechanisms in the stratiform regions appeared to be vapor deposition and aggregation.

In this paper, we extend the study of Churchill and Houze (1984a) beyond the case study of 10 December 1978 by examining the cloud-particle and radar images obtained in all nine cloud clusters that were penetrated by the aircraft at the 7–8 km level. In this effort we seek to determine whether the hydrometeors observed in cloud clusters throughout Winter MONEX were similar in concentration, size, type and growth mechanism to those observed on 10 December 1978. The goal of this research is to document insofar as possible the microphysical structure of equatorial cloud clusters. This paper is not a definitive study of microphysical processes themselves but rather an attempt to determine how microphysical features such as particle structures, concentrations, sizes and growth mechanisms are distributed spatially within the tropical cloud cluster. Houze *et al.* (1981b) and Churchill and Houze (1984a) have shown that Winter MONEX cloud clusters exhibited mesoscale structures and life cycles strikingly similar to those of GATE cloud clusters (observed over the tropical Atlantic). This similarity suggests that whatever microphysical structure can be gleaned from Winter MONEX data is applicable to tropical oceanic cloud clusters in general.

Since Winter MONEX was not designed as a cloud-physics or mesoscale experiment, the set of data is incomplete and the final picture that emerges from the present study is correspondingly fragmentary. Nevertheless, the data obtained constitute a major improvement in our knowledge of the microphysics of tropical cloud clusters: from none to some. Thus this paper reports on the synthesis of a partial data set; however, it provides more insight into tropical cloud cluster microphysics than heretofore available and points the way to future experiments, which can be designed to provide a more complete microphysical picture.

## 2. Data and methods of analysis

Digitized particle images were obtained on board the WP-3D aircraft with the two-dimensional PMS

probes. These probes were developed by Knollenberg (1970), and various aspects of their operation, characteristics and uses have been discussed by Heymsfield (1976), Cannon (1979) and Houze *et al.* (1981a). In this study, we use data from the “cloud probe,” which detected particles up to 1.6 mm in dimension.

Descriptions of the particle data and methods used to analyze them are given in the Appendix of Churchill and Houze (1984a). In the present study we followed the same procedures, so we will only summarize them briefly here. The particle images on magnetic tape represented 2 s average particle concentrations along the flight track. Two seconds is the frequency with which observations were recorded by the PMS data system. The 2 s concentration averages were obtained by counting the number of particles observed in each 2 s period, and dividing by the volume of air which passed through the probe during that period, using the air speed of the P3 as the rate of flow of air through the probe.

From the 2 s average concentrations we arithmetically calculated 1 min average concentrations (1 min of flight time corresponds to about 10 km in horizontal distance travelled). Microfilm images of all the particles sampled were generated from the data tapes. For each minute of flight time, approximately 30 images on microfilm were selected objectively for visual examination. Each particle examined was classified according to size and type. The size categories were *small* (0.1–0.5 mm in dimension), *medium* (0.5–1.2 mm) and *large* ( $>1.2$  mm). The categories of type were *columns*, *branched crystals*, *nearly round particles*, and particles of *indeterminable* shape. Examples of images in each size and type category are given in Fig. A2 of Churchill and Houze (1984a).

In classifying the particle types, we assumed that all the medium and large particles were ice. These particles had sufficient size relative to the resolution of the PMS cloud probe that we could unambiguously determine their phase. Liquid cloud particles in this size range, as evident from PMS images obtained during Winter MONEX in flights through rain, had distinct oblong smooth-edged shapes, and the absence of such shapes in the cells at the 7–8 km level lead us to conclude that the medium and large particles were all ice.

It remains an open question whether or not the small indeterminable particles could have been liquid rather than ice; they were too small relative to the resolution of the cloud probe to permit unambiguous identification. Although the Johnson–Williams (JW) device detects only droplets with radii less than about 50 microns, these data are an indicator of whether or not liquid particles were likely to have been present in the size range sampled by the PMS cloud probe. In all of the “weak” and “very weak” stratiform precipitation (see below for definitions) the JW liquid water contents were zero; hence we assume that none of the small indeterminable particles in these regions

were liquid. In convective and strong stratiform regions, the JW liquid water contents never exceeded  $0.2 \text{ g m}^{-3}$ . These low values suggest a paucity of liquid droplets. Nevertheless, we draw no conclusions that require knowledge of the phases of the small particles sampled by the cloud probe.

The particle concentrations, types and sizes determined by the above methods were stratified by Churchill and Houze (1984a) according to whether the precipitation through which the aircraft was flying was *convective*, *strong stratiform* or *weak stratiform*. The distinction between convective and stratiform was made subjectively on the basis of the appearance of radar echo detected by the C-band (5 cm wavelength) lower fuselage radar aboard the WP-3D aircraft. (Characteristics of this radar are given by Houze *et al.*, 1981a.) The distinction between weak and strong stratiform precipitation was made objectively, according to whether the reflectivity factor was less than or greater than 20 dBZ, respectively, in the vicinity of the aircraft. In the present paper, we follow the same procedures, except that we have identified a further precipitation category, *very weak stratiform*, which refers to precipitation too weak to be detected by the lower fuselage radar (less than about 1 dBZ), but in which precipitation particles were observed.

The size of the data sample we have used is indicated in Table 1, which lists the dates, times, altitudes and types of precipitation encountered for all the penetrations included in this study.

### 3. Concentrations of particles

The one-minute average particle concentrations observed on all of the flights through the four identified categories of precipitation are summarized in histograms in Fig. 1a. The data for the stratiform categories are replotted in Fig. 1b in histograms using a smaller size increment.

In Fig. 1a, all of the observed particle concentrations were less than 50 per liter in very weak stratiform precipitation. The weak stratiform precipitation was rather similar; 98% of the concentrations were less than 50 per liter. However, occasional concentrations of 50–100 per liter occurred. In the strong stratiform precipitation, the occurrence of concentrations of 50–100 per liter became much more frequent (14% of the samples), and occasional concentrations of over 100 per liter were observed. In convective cells, concentrations of over 100 per liter were quite common; 43% of the samples were in the 100–300 per liter range. Thus, a systematic trend of decreasing frequency of low concentrations and increasing frequency of high concentrations was seen in progressing from weaker stratiform to stronger stratiform to convective precipitation.

The distributions of particle concentrations in the stratiform regions are seen with more precision in Fig. 1b. Very similar distributions occurred in the

TABLE 1. Summary of Winter MONEX flights on which this study is based. The aircraft used was a NOAA WP-3D. Types of precipitation are convective (CV), strong stratiform (SSF), weak stratiform (WSF), and very weak stratiform (VWSF).

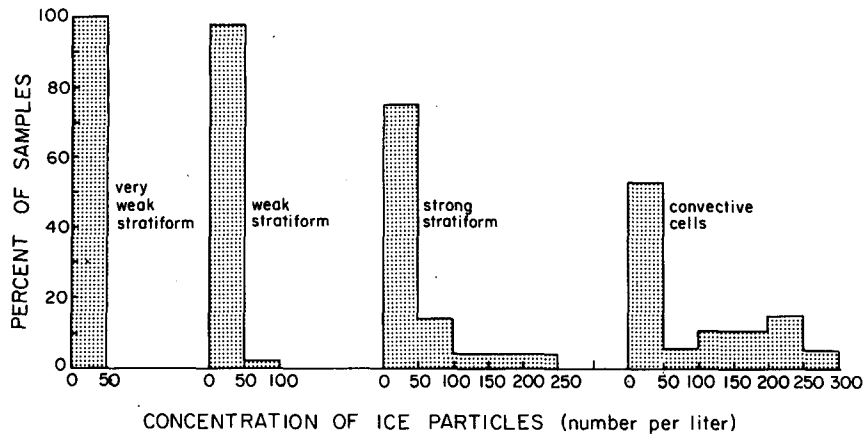
Date (1978)	Time period (GMT)	Altitude range (m)	Type of precipitation
7 December	1028–1031	7354–7361	CV
	1119–1122	7356–7357	SSF
10 December	0905–0910	7214–7434	CV
	0940–1012	7352–7360	WSF
	1031–1041	7351–7360	SSF
	1042–1045	7356–7359	WSF
11 December	0954–0958	7345–7512	CV
	1001–1011	7338–7375	SSF
	1031–1101	7364–7375	WSF
12 December	1004–1007	7352–7358	CV
	1017–1053	7352–7361	WSF
16 December	0930–0935	7354–7357	VWSF
	0951–1009	7352–7360	VWSF
	1010–1019	7346–7365	WSF
17 December	0541–0558	7339–7343	SSF
	0600–0602	7350–7383	CV
	0612–0619	7350–7354	WSF

very weak and weak stratiform regions, where nearly all concentrations were less than 10 per liter. Only a few samples of over 20 per liter were observed in the weak stratiform precipitation. A quite different type of distribution occurred in the strong stratiform regions, where the observed concentrations were spread fairly evenly over the range of 0–70 per liter. Some of the occasional samples of over 100 per liter in the strong stratiform category were found in the vicinity of active convective cells.

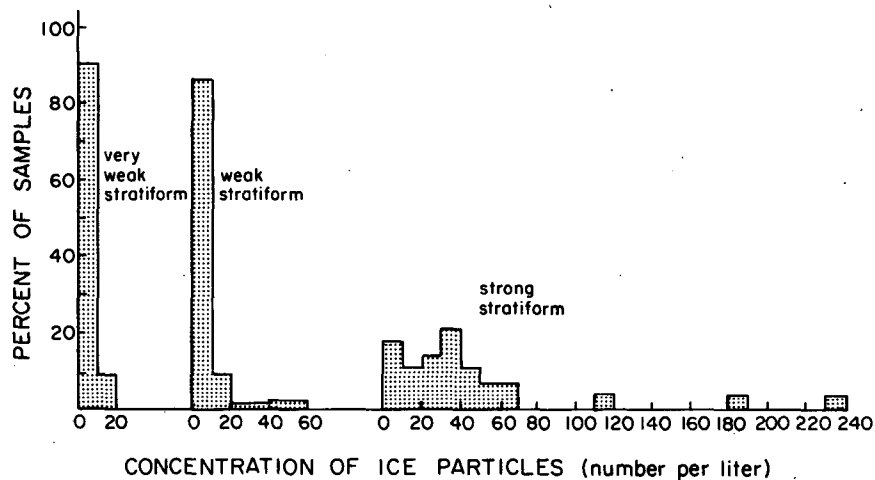
The dominance of concentrations of less than 10 per liter in the weaker stratiform categories and 20–70 per liter in the strong stratiform precipitation agrees with the results obtained by Churchill and Houze (1984a) for the 10 December case study.

### 4. Types and sizes of particles

The types and sizes of particles identified by visual examination of the particle images on microfilm are summarized in Table 2. In convective precipitation (Table 2a), there was never any evidence of columns or branched crystals. A few nearly round particles (probably graupel or frozen drops) were seen. However, most particles (99.0%) were of indeterminate shape, and most of these (90.4% of the total sample) were in the small size category. This distribution is similar to that found for convective cells by Churchill and Houze (1984a) in the 10 December case study. In convective cells, growth of particles by riming is expected because of the high condensation rates and rapid growth of particles in convective clouds (Houghton, 1968); our observed distribution does not



(a)



(b)

FIG. 1. Concentrations of particles observed with the PMS cloud probe (upper particle size limit 1.6 mm) aboard the NOAA WP-3D aircraft during Winter MONEX. Observations were made at altitudes of 7-8 km ( $-14$  to  $-19^{\circ}\text{C}$ ) and the concentrations referred to were 1 min averages. The categories very weak stratiform, weak stratiform, strong stratiform and convective cells describe the precipitation through which the aircraft was flying. In (a) an increment of 50 per liter on the abscissa was used in plotting the histograms. In (b) an increment of 10 per liter was used to show more detail in the stratiform categories.

contradict this expectation. The absence of pristine crystal shapes suggests either that growth by vapor deposition was not effective or the crystals were too small to be identified.

There are several possible explanations for the observed high concentrations of small hydrometeors (greater than 100 per liter) in the convective cells (Fig. 1a). The particles could be supercooled water droplets; however, as noted above, low liquid water contents suggest that ice particles dominated the data. It is further reasonable to assume the small particles were predominantly solid since many other studies have found high concentrations of ice particles in convective cells (e.g., Mossop *et al.*, 1967; Mossop and Ono, 1969; Hallett *et al.*, 1978). The convective

regions penetrated by the P3 were associated with strong updrafts and downdrafts (vertical velocities greater than  $2 \text{ m s}^{-1}$ ). The high concentrations of small particles in these regions could be explained either by ice being generated at low levels and lifted to flight level by convective updrafts or by nucleation of ice particles at lower temperatures above flight level and subsequently lowered to flight level by downdrafts. However, at the flight levels where the data were collected, the convective regions of the clusters penetrated by the aircraft were characterized more by updrafts than downdrafts (Fig. 2), which suggests that the dominant effect is the updraft lifting particles to flight level, rather than downdrafts bringing them down from above.

TABLE 2. Frequency distribution of ice particles in size and type for convective precipitation, strong stratiform, weak stratiform and very weak stratiform during Winter MONEX. Numbers indicate the percentage of particles sampled for each kind of precipitation. Small particles were less than 0.5 mm in dimension, medium particles were 0.5–1.2 mm, and large particles were >1.2 mm.

	Columns	Branched crystals	Indeterminable	Nearly round
(a) Convective				
Small	0	0	90.4	0.8
Medium	0	0	6.2	0.1
Large	0	0	2.4	0.1
(b) Strong Stratiform				
Small	0.3	0	60.2	0
Medium	1.3	0	32.4	0.1
Large	0	0.1	5.5	0.1
(c) Weak Stratiform				
Small	1.4	0.1	55.4	1.7
Medium	2.5	2.6	26.4	0.3
Large	0.3	2.6	6.8	0
(d) Very Weak Stratiform				
Small	0	0	72.7	0
Medium	0	0.3	24.8	0
Large	0	0	2.2	0

With the supposition that the particles generally were associated with updrafts, it becomes apparent that nucleation of ice at lower warmer levels cannot account for the high concentrations. The number of ice nuclei per liter at a given temperature is given approximately by the formula,

$$N = \exp[a(-20 - T)], \quad (1)$$

where  $T$  is the temperature ( $^{\circ}\text{C}$ ),  $a$  has a value of about 0.3, and  $N$  is the number of nuclei (Eq. 10.1, p. 632, Hobbs, 1974). At a temperature of  $-17^{\circ}\text{C}$ , which is a typical value for these flights, the expected nuclei concentration is 0.41 particles per liter, which is three orders of magnitude smaller than the number observed in the convective cells.

These concentrations alternatively could be explained by ice multiplication processes in cloud at temperatures of  $-3$  to  $-8^{\circ}\text{C}$  (about the 5–6 km level in Winter MONEX). At such temperatures supercooled droplets splinter as they freeze on contact with ice particles, resulting in larger numbers of small ice particles (Hallett and Mossop, 1974; Mossop and Hallett, 1974; Mossop, 1976, 1978). So we conjecture that the most likely mechanisms resulting in the observed high particle concentrations is ice multiplication at the 5–6 km level with strong updrafts lifting the particles to flight level (7–8 km).

The size–type distribution for particles in strong stratiform precipitation (Table 2b) has characteristics

that are transitional between the convective cells (Table 2a, just discussed) and weak stratiform precipitation (Table 2c, to be discussed below). This result is similar to that of 10 December (Churchill and Houze, 1984a), when strong stratiform precipitation was generally found near active or recently active convective cells. This type of precipitation apparently consisted of a mixture of debris from convection and purely stratiform precipitation particles.

The particles in weak stratiform precipitation differed sharply from those seen in convective cells (compare Tables 2a and c). Pristine crystalline shapes (i.e. columns and branched crystals) were much in evidence in the weak stratiform precipitation, whereas they were completely lacking in the convective cells. Thus, growth by vapor deposition, not apparent in the convection, was present in the weak stratiform regions. Another major difference between the convection and the weak stratiform precipitation is in the size distribution of indeterminable particles. In the convective cells, the indeterminable particles were nearly all small. However, in the weak stratiform regions, small indeterminable particles accounted for only about 55% of the total sample, while the medium-sized indeterminable particles accounted for about one-fourth of the total.

The tendency of indeterminable particles in the weak stratiform precipitation to have sizes larger than in convective precipitation suggests either that many of the weak-stratiform indeterminable particles were aggregates, or that the stratiform particles were older and had more time to grow to larger sizes. The flight

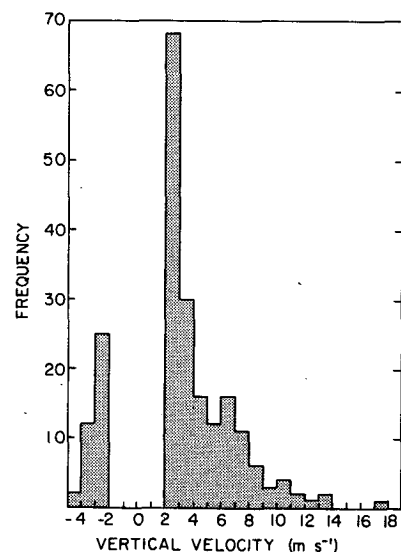


FIG. 2. Histogram of vertical velocities of magnitude greater than  $2 \text{ m s}^{-1}$  in the convective regions penetrated by the P3 during Winter MONEX. Based on 1 s averaged data. Note that no downdrafts of magnitude greater than  $5 \text{ m s}^{-1}$  were observed, while numerous updrafts of this magnitude were observed. Values between  $-2$  and  $+2 \text{ m s}^{-1}$  were omitted, as this is the approximate noise range of P3 vertical velocities during Winter MONEX.

level temperature range ( $-14$  to  $-19^{\circ}\text{C}$ ) is within the range of temperatures at which aggregates have been observed (see Fig. 10.4, p. 641 of Hobbs, 1974). Many of the indeterminate particle images had the appearance ascribed by Heymsfield and Musil (1982) to aggregation of ice particles. However, the shadowgrams provided by the PMS probes do not allow unambiguous identification of aggregates; therefore, the presence of aggregation must be considered consistent with but not conclusively shown by the data.

The small nearly round particles seen in 1.7% of the weak stratiform samples may have been branched crystals or aggregates whose true structure, because of their small size, either could not be adequately resolved by the PMS probe or could not be adequately portrayed in our microfilm output. These particles were not generally perfectly round, like a frozen drop, and since no cloud liquid water was detected at flight level in any of the weak stratiform, it is unlikely that these were rimed particles or drops. The small nearly round particles in weak stratiform precipitation were often accompanied by columns, so it may have been that the nearly round particles were columns being seen on end, as the columns assumed random orientations while passing through the probe.

The size-type distribution for particles in weak stratiform precipitation (Table 2c) is similar to that found on 10 December by Churchill and Houze (1984a). We conclude, as before, that the observed particles indicated particle growth by vapor deposition and probably aggregation and that the presence of branched crystals at flight level indicated growth at water saturation at altitudes above 8 km (where temperatures were  $-20$  to  $-25^{\circ}\text{C}$ ). The stratiform regions penetrated by the aircraft commonly extended over distances of 100–300 km (corresponding to penetration times of 10 to 30 min, see Table 1). The water saturation must have been produced by mesoscale ascent that was strong enough across these regions to produce the saturation but weak enough to allow the particles to fall to flight level. Mesoscale ascent of this character at upper levels is consistent with conceptual models of the stratiform regions of tropical cloud clusters (Houze and Betts, 1981; Houze and Hobbs, 1982; Houze, 1982) and with various modeling and diagnostic studies of the stratiform regions of tropical cloud clusters (Brown, 1979; Leary and Houze, 1979; Gamache and Houze, 1982; Johnson, 1982; Houze and Rappaport, 1984; Churchill and Houze, 1984b). The Johnson (1982) and Churchill and Houze (1984b) studies, using different approaches, diagnosed mesoscale updraft motion at upper levels in the stratiform region of one of the 10 December 1978 Winter MONEX cloud clusters.

In the very weak stratiform precipitation (Table 2d), the size-type distributions resembled those of the weak and strong stratiform precipitation in that about 25% of the particles were in the medium-size, indeterminate-shape category. However, there were

more smaller particles (72.7%) than in the other two stratiform categories, and there was very little evidence of columnar or branched crystalline structure (zero in all column and branched categories except for 0.3% in the medium-sized branched category). No nearly round particles were seen. Evidently, the very weak stratiform precipitation was associated with dissipating stratiform regions, where larger particles had generally fallen out without being replenished, since convection was absent and mesoscale updraft activity and concomitant particle growth had weakened or ceased. The near-absence of branched crystals (which grow at water saturation) further indicated decreased updraft motion. Without upward motions in the cloud, evaporation may have contributed along with fallout to the decreased sizes of particles.

## 5. Conclusions

Images of hydrometeors in the size range 0.1 to 1.6 mm obtained aboard an aircraft flying at the 7–8 km ( $-14$  to  $-19^{\circ}\text{C}$ ) level in tropical cloud clusters over the South China Sea have been analyzed by stratifying the data according to radar observations of the type of precipitation in which the particle images were obtained.

In convective precipitation areas, 1 min average particle concentrations of 100–300 per liter were found frequently. We speculate that ice multiplication may have been active in the convection at lower levels. However, ambiguity about the phase of the small-particle images prevents this from being a definite conclusion.

An absence of vapor-grown ice particles and aggregates indicated that riming was the dominant particle growth mechanism in convection. Riming and the production of high ice-particle concentrations are typical features of convective clouds observed elsewhere; thus, in this respect the convection in tropical cloud clusters appears microphysically to be rather normal.

Strong stratiform precipitation (i.e., stratiform precipitation with radar reflectivity greater than 20 dBZ) had typical particle concentrations of 20–70 per liter, with occasional values over 200 per liter. These occasional high concentrations, together with the observed types and sizes of particles, indicated that the strong stratiform precipitation, typically found near active convection, was a mixture of debris from convective cells and particles grown in a more stratiform environment.

The weak stratiform precipitation (radar echo intensity between 1 and 20 dBZ) exhibited microphysical structure decidedly different from that seen in the convective areas. Nearly all observed concentrations of particles (86%) were less than 10 per liter. Vapor grown particles (i.e. columns and branched crystals) were present, and the indeterminate-shaped particles had sizes and general appearances suggesting

they were aggregates of crystals. These particle structures and apparent growth mechanisms are consistent with the presence of the weak mesoscale ascent reported by Gamache and Houze (1982), Johnson (1982) and Churchill and Houze (1984b) to be located in the upper levels of the stratiform regions of tropical cloud clusters. Thus we conclude that the stratiform regions of tropical cloud clusters, previously recognized only by their radar-echo, wind and thermodynamic fields, have a corresponding physically consistent cloud microstructure, characterized by hydrometeor growth processes that are clearly distinguishable from those of convective regions.

In very weak stratiform precipitation (not detectable by the airborne radar), particle characteristics suggested dissipating stratiform cloud structure, in which mesoscale updraft motion had weakened or ceased.

*Acknowledgments.* We are indebted to Professor Lawrence F. Radke who, as cloud physics scientist aboard the WP-3D aircraft during Winter MONEX, insured the collection of high quality particle image data on which this study was based. We also thank Mr. Abhik Biswas for carrying out the extensive data reduction and tabulation required for this study. Dr. Paul Herzegh provided us with software for processing the PMS data. Professor Peter V. Hobbs, Mr. John Locatelli, Mr. Art Rangno and our *JAS* reviewers provided helpful comments in interpreting particle images and results. Figures were drafted by Ms. Kay Moore. This research was supported by the National Science Foundation, Grant ATM80-17327.

#### REFERENCES

- Austin, P. M., and S. G. Geotis, 1979: Raindrop sizes and related parameters for GATE. *J. Appl. Meteor.*, **18**, 569-575.
- Brown, J. M., 1979: Mesoscale unsaturated downdrafts driven by rainfall evaporation: A numerical study. *J. Atmos. Sci.*, **36**, 313-338.
- Cannon, 1979: Imaging devices. *Atmos. Technol.*, **8**, 32-37.
- Churchill, D. D., and R. A. Houze, Jr., 1984a: Development and structure of winter monsoon cloud clusters on 10 December 1978. *J. Atmos. Sci.*, **41**, 933-960.
- , and —, 1984b: Mesoscale updraft magnitude and cloud-ice content deduced from the ice budget of a tropical cloud cluster. *J. Atmos. Sci.*, **41**, 1717-1725.
- Cunning, J. B., and R. I. Sax, 1977: A Z-R relationship for the GATE B-scale array. *Mon. Wea. Rev.*, **105**, 1330-1336.
- Gamache, J. F., and R. A. Houze, Jr., 1982: Mesoscale air motions associated with a tropical squall line. *Mon. Wea. Rev.*, **110**, 118-135.
- , and —, 1983: Water budget of a mesoscale convective system in the tropics. *J. Atmos. Sci.*, **40**, 1835-1850.
- Hallett, J., and S. C. Mossop, 1974: Production of secondary ice particles during the riming process. *Nature*, **249**, 26-28.
- , R. I. Sax, D. Lamb and A. S. R. Murty, 1978: Aircraft measurements of ice in Florida cumuli. *Quart. J. Roy. Meteor. Soc.*, **104**, 631-651.
- Heymsfield, A. J., 1976: Particle size distribution measurement: An evaluation of the Knollenberg optical array probes. *Atmos. Technol.*, **8**, 17-24.
- , and D. J. Musil, 1982: Case study of a hailstorm in Colorado. Part II: Particle growth processes at mid-levels deduced from *in situ* measurements. *J. Atmos. Sci.*, **39**, 2847-2866.
- Hobbs, P. V., 1974: *Ice Physics*, Clarendon Press, 863 pp.
- Houghton, H. G., 1968: On precipitation mechanisms and their artificial modification. *J. Appl. Meteor.*, **7**, 851-859.
- Houze, R. A., Jr., 1977: Structure and dynamics of a tropical squall-line system observed during GATE. *Mon. Wea. Rev.*, **105**, 1540-1567.
- , 1982: Cloud clusters and large-scale vertical motions in the tropics. *J. Meteor. Soc. Japan*, **60**, 396-414.
- , and A. K. Betts, 1981: Convection in GATE. *Rev. Geophys. Space Phys.*, **19**, 541-576.
- , and P. V. Hobbs, 1982: Organization and structure of precipitating cloud systems, *Advances in Geophysics*, Vol. 24, Academic Press, 225-315.
- , and E. N. Rappaport, 1984: Air motions and precipitation structure of an early summer squall line over the eastern tropical Atlantic. *J. Atmos. Sci.*, **41**, 553-574.
- , S. G. Geotis, F. D. Marks, Jr., D. D. Churchill and P. H. Herzegh, 1981a: Comparison of airborne and land-based radar measurements of precipitation during winter MONEX. *J. Appl. Meteor.*, **20**, 772-783.
- , —, and A. K. West, 1981b: Winter monsoon convection in the vicinity of North Borneo. Part I: Structure and time variation of the clouds and precipitation. *Mon. Wea. Rev.*, **109**, 1595-1614.
- Johnson, R. H., 1982: Vertical motion of near-equatorial winter monsoon convection. *J. Meteor. Soc. Japan*, **60**, 682-690.
- Knollenberg, R. G., 1970: The optical array: An alternative to scattering or extinction for airborne particle size determination. *J. Appl. Meteor.*, **9**, 86-103.
- Leary, C. A., 1980: Temperature and humidity profiles in mesoscale unsaturated downdrafts. *J. Atmos. Sci.*, **37**, 1005-1012.
- , 1984: Precipitation structure of the cloud clusters in a tropical easterly wave. *Mon. Wea. Rev.*, **112**, 313-325.
- , and R. A. Houze, Jr., 1979: Melting and evaporation of hydrometeors in precipitation from the anvil clouds of deep tropical convection. *J. Atmos. Sci.*, **36**, 669-679.
- Mossop, S. C., 1976: Production of secondary ice particles during the growth of graupel by riming. *Quart. J. Roy. Meteor. Soc.*, **102**, 45-56.
- , 1978: The influence of drop size distribution on the production of secondary ice particles during graupel growth. *Quart. J. Roy. Meteor. Soc.*, **104**, 323-330.
- , and A. Ono, 1969: Measurements of ice crystal concentrations in cloud. *J. Atmos. Sci.*, **26**, 130-137.
- , and J. Hallett, 1974: Ice crystal concentration in cumulus clouds: Influence of the drop spectrum. *Science*, **186**, 632-634.
- , A. Ono, and K. J. Heffeman, 1967: Studies of ice crystals in natural clouds. *J. Rech. Atmos.*, **1**, 45-64.